12-2022

The Molecular Evolution of Insect Opsin Genes

Maria Jose Cardenas Muedano
The University of Texas Rio Grande Valley

THE MOLECULAR EVOLUTION OF INSECT OPSIN GENES

A Thesis

by

MARIA JOSE CARDENAS MUEDANO

Submitted in Partial Fulfillment of the

Requirements for the Degree of

MASTER OF SCIENCE

Major Subject: Biology

The University of Texas Rio Grande Valley

December 2022

THE MOLECULAR EVOLUTION OF INSECT OPSIN GENES

A Thesis
by
MARIA JOSE CARDENAS MUEDANO

COMMITTEE MEMBERS

Dr. Matthew Terry
Chair of Committee

Dr. Michael Persans
Committee Member

Dr. Megan Keniry
Committee Member

December 2022

ABSTRACT

Cardenas Muedano, Maria Jose. The Molecular Evolution of Insect Opsin Genes. Master of Science (MS), December, 2022, [Page Number for Biographical Sketch] pp., 1 table, 15 figures, references, [total # of titles in REFERENCES] titles.

Opsins are part of the superfamily of G-coupled receptor proteins and together with chromophores, are responsible for initiating the signal transduction cascade responsible for animal vision. Since opsins have a critical role on visual perception these genes are crucial for a myriad of adaptive traits and behaviors and should show diverse signs of natural selection at the molecular level. Understanding the evolution of opsins across the wide diversity of insect groups will allow us to better understand the evolutionary pressure on insect opsins and serve as a model for both other gene systems and other taxonomic groups of animals that are more difficult to study.

Our goal was to expand our sampling of insect opsins and then use these new data to explore and better understand patterns of evolution and diversity of these crucial genes. Moreover, we performed a spatial localization of opsin expression in the compound eye of a species of praying mantis native to the Rio Grande Valley, *Bistanta mexicana*.

DEDICATION

The completion of my graduate studies would not have been possible without the love and patience of my brilliant wife Clarissa Mae de Leon. Thank you for never giving up on me.

Aunque no estás aquí conmigo para celebrar, espero que veas esto desde donde estés Ma. ¡Esto va por ti!

ACKNOWLEDGMENTS

Undertaking my graduate studies during the COVID-19 pandemic was challenging, and there were moments in which I almost gave up. However, I will always be grateful to Dr. Matthew Terry, chair of my dissertation committee, for all his mentoring and advice. He took me under his wing and made sure we finished this project no matter how many obstacles we faced. My thanks go to my dissertation committee members: Dr. Michael Persans, and Dr. Megan Keniry. Their advice, input and comments on my dissertation helped to ensure the quality of my intellectual work. Special thanks go to Dr. Persans and Dr. Robert Dearth, who always encouraged me to continue with my studies and pursue a doctoral degree: I will keep my promise!

I would also like to thank my colleagues at the UTRGV Biology department. My wife Clarissa Mae de Leon, who captured all the insect specimens I was too afraid to catch and helped me process the transcriptome data for this project. Tripti Saini, who helped me process supporting confocal microscopy data for my research. And Sakshi Watts, who was an inspiring force throughout this endeavor and an encouraging friend. Eleazar Saenz has been an incredibly caring mentor and Julie Perez brings sunshine into everyone's day.

Finally, I am immensely grateful to the R & K Dugger endowment, which allowed me to perform my research on fauna native to the Rio Grande Valley.

TABLE OF CONTENTS

Page

LIST OF TABLES

Page

LIST OF FIGURES

Page

CHAPTER I

OVERVIEW OF COMPLEX EYES

Although photosensitivity is an ancestral feature of all Bilateria paired image forming organs (complex eyes) have evolved independently multiple times in Metazoa. These intricate structures are made up of multiple cell and tissue varieties that, through the process of morphogenesis, develop precise structures and arrangement of those structures to support various visual functions (Koenig and Gross, 2020).

Previously, it was considered that complex eyes had occurred in three separate events within Metazoa through convergent evolution (Erclik et al., 2009). However, it is now understood that at their most fundamental level the different types of metazoan eyes have a deep connection and homology (Koenig and Gross, 2020). The three major representations of complex eyes in metazoans are vertebrates, cephalopods, and arthropods, all of which share key ancestral components that enable specific visual functions (Fig. 1). There are some obvious morphological similarities between these three types of complex eyes, with the vertebrate and cephalopod eyes being the most morphologically similar. In the vertebrate and cephalopod eyes, a single lens is present in the anterior and a retina is present in the posterior. In addition, a pigment layer must be present behind or inside the retina, and the cornea is frequently located anterior to the lens (Koenig and Gross, 2020).

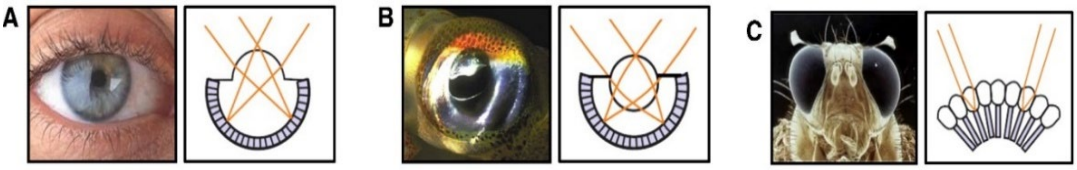

Figure 1. Diversity of Complex Eyes within Metazoa.

(A) The human eye is an example of a single-chambered vertebrate eye with corneal optics that integrate nerve, muscle, and connective tissues. The vertebrate eye evolved very early in chordates. (B) Cephalopods such as the squid also have single-chambered eyes, but their refractive lens is rather static, so the length of the eye itself is what changes for the cephalopod to focus the image. Additionally, the opsins are positioned backwards compared to the vertebrate eyes. (C) Arthropods, such as the fruit fly shown, possess compound eyes that are sensitive to a wide range of wavelengths. Adapted from Erclik et al. (2009).

What is perhaps more interesting is the presence of a developmental connection between these three complex eyes. Prior to the molecular revolution, biologists predicted that complex eyes had evolved independently (convergence) at least 40 times in Metazoa (Koenig and Gross, 2020). However, Quiring et al. discovered that the *Drosophila* gene *eyeless* was a homolog of the human gene aniridia (*PAX6*) and the mouse gene small eye (*Pax6*) (1994). Soon, the retinal determination network (RDN), which includes the genes *eyeless* (*ey*; *Pax6* in mouse), *twin of eyeless* (*toy*; *Pax6* in mouse), *sine oculis* (*so*; *Six1/2* in mouse), *Optix* (*Six3/6* in mouse), *dachshund* (*dac*), and *eyes absent* (*eya*) were added to the list of homologous genes that are directly linked to the development of eyes in other animals (Gehring, 2014). Our view of the evolutionary link between vertebrates and other distantly related organisms has been significantly altered because of this revelation. It implied the existence of ancient genetic networks with a shared connection to animal patterning

and organ development (Koenig et al., 2020). For more than 25 years, this premise has guided research in evolutionary developmental biology. Therefore, the study of the evolution of complex eyes is increasingly significant as an opportunity to decipher the developmental connections within Metazoa.

Insect Compound Eyes

Most arthropods have compound eyes, which are prominent visual organs. The compound eyes of arthropods differ from the single-chambered eyes of vertebrates in that they generally consist of numerous independent optical units termed ommatidia. This morphological difference has implications in the visual performance of these organs and helps to mediate important functions like flight control, navigation, prey capture, predator avoidance, and mate recognition (Chen and Hua, 2016).

The apposition type and the superposition type are the two fundamental optical designs of the compound eyes of arthropods (Fig. 2). Each ommatidium is optically isolated from all others with longitudinal pigments in the apposition type. This means that each ommatidium can be considered and independent image forming structure and that the many nerve signals generated by each of these units must be integrated and processed by the arthropod brain.

All photoreceptors of the superposition type share corneal dioptrical units thanks to the presence of a pigment less clear zone between the cornea and rhabdomeres, and thus the eye is more sensitive to light (Chen and Hua, 2016). Superposition eyes are frequently seen in nocturnal insects, though they can also be seen in some diurnally active insects (Chen and Hua, 2016).

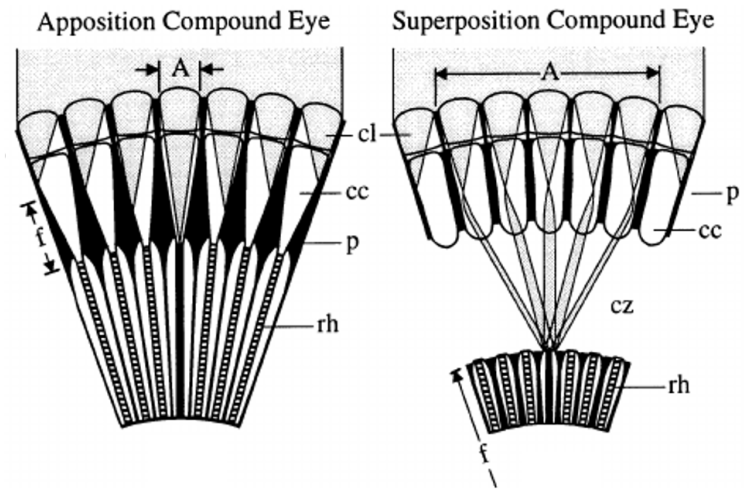

Figure 2. Designs of insect compound eyes.

The directions and outcomes of parallel light rays impacting on the surface of the external eye are shown in the shaded area. The target photoreceptor is colored black in each design. The aperture's diameter is *A*, the focal length is *f*, the crystalline cones are *cc*, the cornea is *co*, the screening pigment is *p*, the rhabdom is *rh*, the photoreceptor is *ph*, the clear zone is *cz*, and the lens is *l*. In superposition eyes, the focal length is measured from the eye's center of curvature (not shown). Adapted from Warrant and Locket (2004).

CHAPTER II

PHOTORECEPTORS

The Golden Trio: Photoreceptors at the Molecular Level

The golden trio of photoreceptors are rhodopsin, chromophore (retinal) and G protein. I will briefly describe them to have a better understanding of the structure and function of photoreceptors at the molecular level.

Rhodopsin

"Rhodopsin is a membrane protein that consists of two parts: the apoprotein, termed opsin, and the prosthetic group chromophore, whose presence is responsible for the color of the compound" (Shichida and Matsuyama, 2009). As seen in Fig. 3 the N-terminus of rhodopsin is in the disc membrane lumen (topologically the extracellular side), whereas the C-terminus is located on the cytoplasmic side, forming a distinctive seven transmembrane helix shape (Shichida and Matsuyama, 2009).

Based on sequence homology, opsins belong to the family-A (or rhodopsin-like superfamily) GPCRs (Shichida and Matsuyama, 2009). Rhodopsin is the G-protein couple receptor (GCPR) that has been most thoroughly studied to date, and it serves as a model for understanding

other GPCRs. Given that retinal serves as the ligand for all opsins, it is logical to infer that rhodopsin originated from a retinoid receptor that gained the capacity to covalently connect to its ligand, enabling it to develop into a photoreceptor molecule (Shichida and Matsuyama, 2009). The ancient opsin or opsins eventually underwent a process of diversification by interacting with various G proteins (Fig. 4).

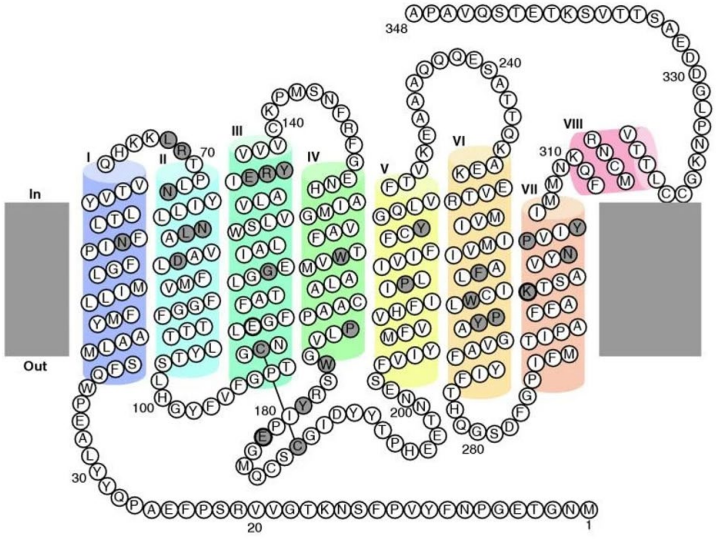

Figure 3. Bovine rhodopsin's secondary structure.

A gray background is used to highlight amino acid residues that are highly conserved throughout the whole opsin family. With bold circles, the counterion position (E113), the retinal-binding site (K296), and the counterion in opsins other than the vertebrate visual and non-visual ones (E181) are all identified. A disulfide bond is formed between C110 and C187. Adapted from Terakita (2005).

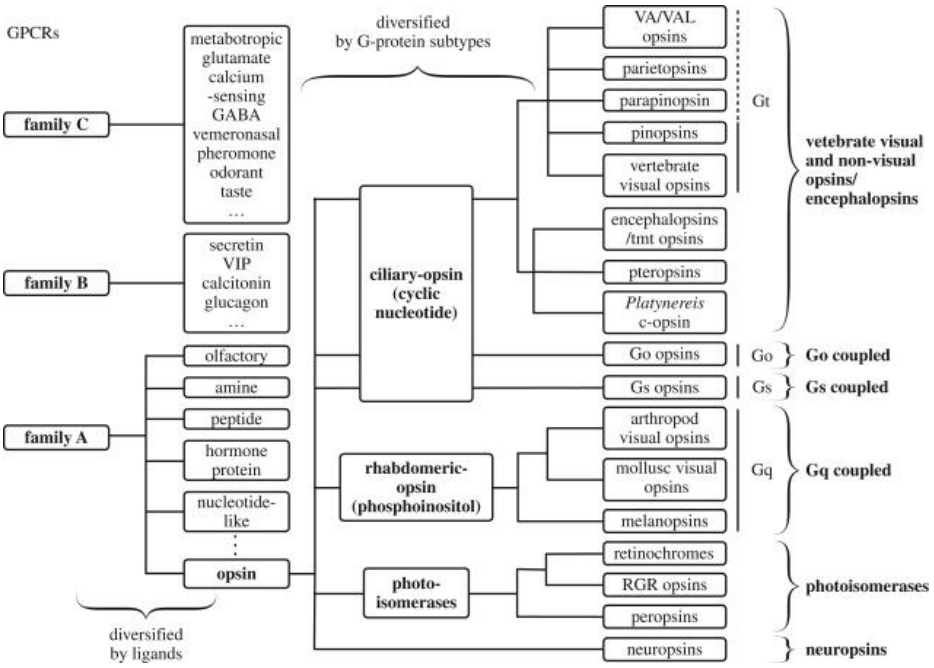

Figure 4. Schematic representation of the phylogenic relationship of opsins.

The schematic phylogenetic tree of GPCRs proposed by Shichida and Matsuyama indicates that GPCRs initially diversified by responding to different ligands, following a diversification based on their response through different G proteins (2009).

Chromophore (retinal)

A retinaldehyde derived from vitamin A, such as retinal (A1), 3,4-dehydroretinal (A2), 3-hydroxyretinal (A3), or 4-hydroxyretinal (A4), makes up the chromophore moiety (Shichida and Matsuyama, 2009). A Schiff base linkage, which can be protonated or unprotonated depending on the environment that a certain opsin provides, is used to covalently bind retina to a lysine residue at helix 7 (H7) (Shichida and Matsuyama, 2009). As a result of the p electrons being delocalized the protonation of the Schiff base, the compound's absorbance shifts to the red, making it capable

of absorbing visible light (Shichida and Matsuyama, 2009). The chromophore is protonated in bovine rhodopsin, which causes it to absorb visible light (Fig. 5).

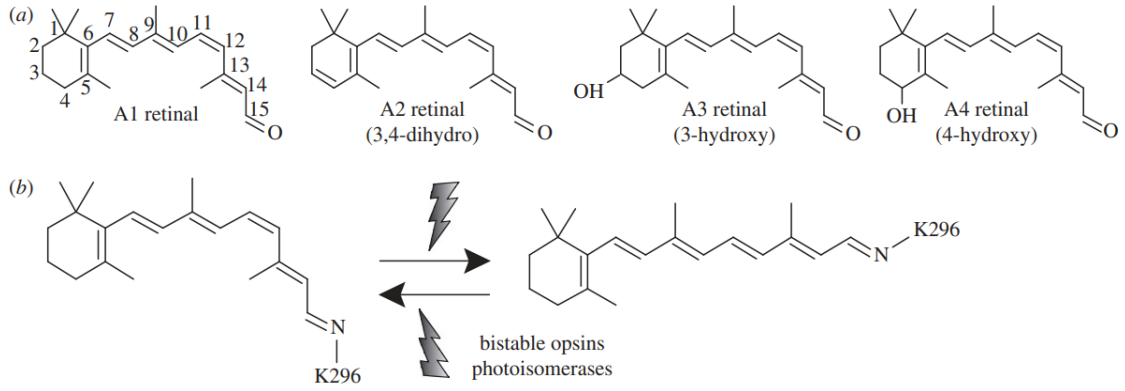

Figure 5. The chromophore: retinal.

(a) Variations in the A1, A2, A3, and A4 retinals that opsins employ. (b) Retinal photoisomerization. In opsins, the retinal is sterospecifically isomerized from 11-cis to all-trans and is covalently linked to a lysine at position H7. When a second photon is absorbed by some opsins, the photoisomerized all-trans-retinal can be transformed back to 11-cis-retinal. There are other photoisomerases, which bind all-trans-retinal to create 11-cis-retinal. Adapted from Shichida and Matsuyama (2009).

G protein

The signal-transducing molecule that mediates and transmits the signal from the light-sensing rhodopsin is known as the G protein (guanine nucleotide-binding protein) or transducin. It is the molecule that converts light impulses into the cell's more recognizable chemical messages (Fig. 6).

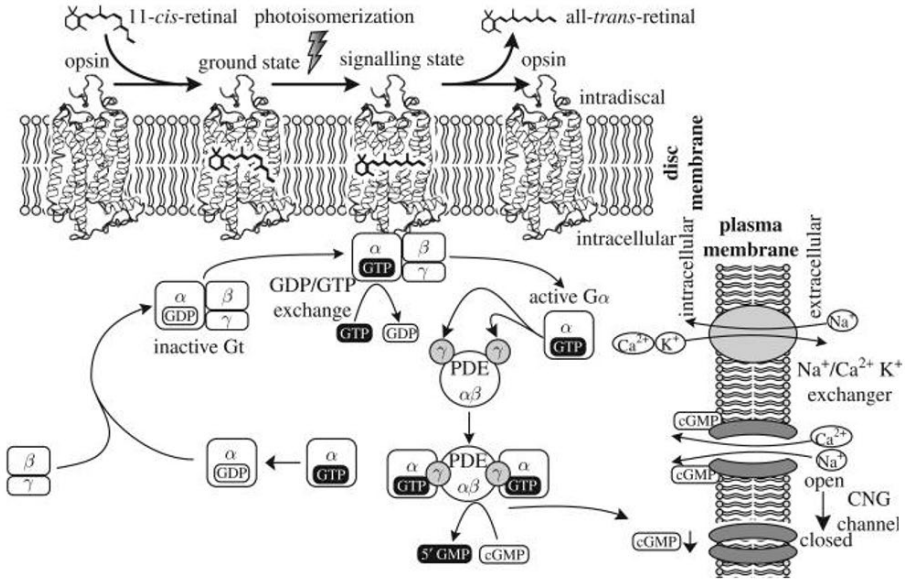

Figure 6. Mechanism of Phototransduction in Mammalian Eyes

Opsins absorb photons to create a signaling state that can connect to the G protein and activate it by catalyzing the conversion of GDP to GTP. When *Gα* dissociates from *Gβγ*, it exposes its active site. Then the activated *Gα* can bind to its effector, PDE (cyclic nucleotide phosphodiesterase) and activate it. The phosphodiester bond of cGMP is broken by PDE, resulting in 50 GMP. As a result of the drop in cGMP concentration, CNG (cyclic nucleotide gated) channels close, causing the photoreceptor cells to become hyperpolarized. Since light-activated rhodopsin is thermally unstable, the chromophore eventually detaches from the opsin. The release of neurotransmitters to downstream cells is modulated by the hyperpolarization of the photoreceptor cell's membrane potential. The light signal travels through many cells before arriving at the ganglion cells that make up the optic nerve and send signals to the brain. Adapted from Shichida and Matsuyama (2009).

Summing up, light sensing is the initial stage of vision, and rhodopsin is the molecule that ‘senses' light by absorbing it (Shichida and Matsuyama, 2009). Rhodopsin undergoes changes in its chemical structure because of light absorption, enabling it to activate the G protein, which then triggers an enzymatic signaling cascade that causes an electrical response in the photoreceptor cell (Shichida and Matsuyama, 2009). Rhodopsin signals are magnified at this stage because a single rhodopsin molecule can activate several G proteins. Furthermore, the G protein subtype affects the downstream signaling cascade because different G proteins can operate in various ways (Shichida and Matsuyama, 2009).

Morphology of Insect Photoreceptors

Previous morphology studies by Chen and Hua (2016) elucidate the complex photoreceptor structure of the insect order *Mecoptera* (Scorpionfly), which will be referred to from now on as a general guide to the morphology of insect compound eyes.

Insect compound eyes, as in all arthropods) are generally composed of numerous independent optical units termed ommatidia (Chen and Hua, 2016). A cornea, crystalline cone, collection of photoreceptors, and basal matrix make up each individual ommatidium (Chen and Hua, 2016). The crystalline cone is located beneath the cornea, and its proximal end is connected to the tips of photoreceptors (Chen and Hua, 2016). Around the crystalline cone, a pair of pigment cells connect to the apical surface of the photoreceptor cluster. In contrast to secondary pigment cells, primary pigment cells often have nuclei that are located closer to the cornea's outer surface (Chen and Hua, 2016). Each ommatidium has eight photoreceptors, which are typically distributed radially along the longitudinal axis (R1–R8). A rhabdomere is made up of the stack of microvilli

that each photoreceptor has (Chen and Hua, 2016). Seven photoreceptors' rhabdomeres (R1–R7) combine to form one rhabdom (Fig. 7). Between the retina and the lamina (the most distal portion of the insect brain), is a structure called the basal matrix. In the eye of *P. dubia* eight ommatidium photoreceptors develop into axons, which bundle up and pass through a circular perforation to the lamina (Chen and Hua, 2016).

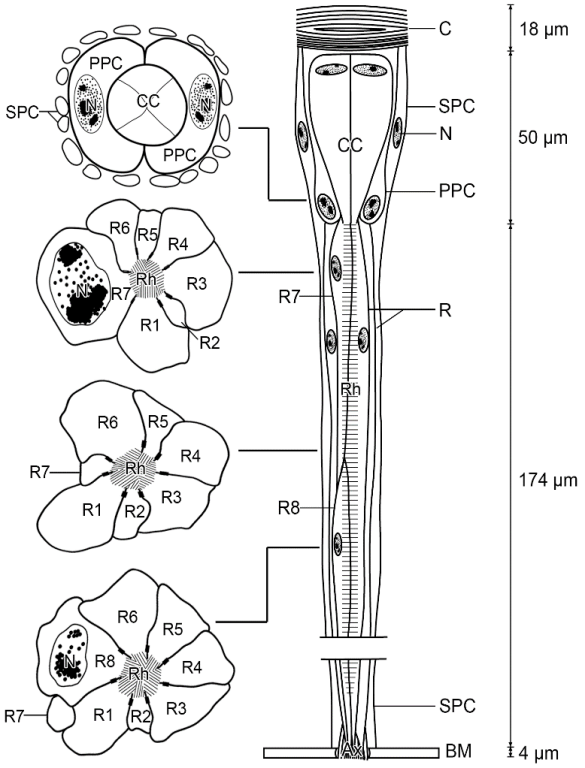

Figure 7. Diagram of the typical cellular architecture of insect ommatidia.

Based on the ommatidium of adult *Panorpa dubia* (*Mecoptera*: Scorpionfly), the longitudinal and four transverse sections can be observed here. *Ax*, axon; *BM*, basal matrix; *C*, cornea; *CC*, crystalline cone; *N*, nucleus; *PPC*, primary pigment cell; *R*, photoreceptor; *Rh*, rhabdom; *SPC*, secondary pigment cell (Chen and Hua, 2016).

CHAPTER III

OPSINS

While the developmental networks governing the formation of complex eyes have been widely studied, such as the comparative evolution studies focused on the retinal determination network (RDN), there is a knowledge gap when it comes to the evolution of visual functions within Metazoa. It is considered that a single homologous photoreceptor developed in early Metazoa and evolved into different complex eyes (Porter et al., 2012). This photoreceptor protein is suspected to be the genetic ancestor of all modern opsin proteins. These proteins play a critical role in the perception of light and serve as the initial point of light absorption that eventually leads to signal transduction. Both the number of different opsins available and their respective expression domains determine the visual spectrum and complexity of signals that can be generated by the eye. This study adds to our understanding of the molecular evolution of opsins across the insects and looks specifically at the expression domains of a subset of these genes in the order *Mantodea* (praying mantises), looking specifically and *Bistanta mexicana*, a species of mantis that ranges from central Mexico to the southern United States. As opsin genes are crucial for a myriad of adaptive traits and behaviors and we anticipate diverse signs of natural selection at the molecular level and in the patterns of opsin expression in the insect eye.

Opsins: G-Coupled Receptors

Opsins are members of the G-protein coupled receptor (GPCR) superfamily, proteins with seven transmembrane helices that are engaged in a wide range of signaling processes (Porter et al., 2012). The opsins are a sizable monophyletic subclass of proteins that belong to the GPCR superfamily. Moreover, some opsin subfamilies are also expressed in non-visual photoreceptor cells but are still involved in signal transduction cascades (Terakita, 2005). Those opsins involved in signaling transduction pathways allowing light sensitivity will be referred to as "visual opsins", while those opsins involved in non-visual pathways will be simply referred to as "non-visual opsins". Previous research has shown that arthropod visual opsins can be divided into three main groups: short-wavelength (SW) opsins that are sensitive to UV light, middle-wavelength (MW) opsins that are sensitive to blue light, and so-called long-wavelength (LW) opsins whose spectral sensitivities are more variable and range from blue-violet to infrared (Henze et al., 2012).

Visual opsins are covalently bound to a chromophore (typically an aldehyde derived from vitamin A). A lysine acts as the chromophore's attachment point in the seventh transmembrane helix of visually functional opsins (Porter et al., 2012). Together, the opsin protein and the chromophore form the visual pigment molecule, which is considered the basic unit of visual perception in animals (Porter et al., 2012).

Opsin Diversity Across the Animal Kingdom

Opsins can be divided into four main monophyletic groups: those from ciliary photoreceptors (also known as C-opsins), those from rhabdomeric photoreceptors (also known as R-opsins), those from cnidarian photoreceptors (also known as Cnidops), and a mixed group made

up of retinal G-protein coupled receptors (RGR), peropsins and neuropsins (also known as Group 4 opsins) (Porter et al., 2012). Knowing the important duplication and diversification events that have produced the diversity of opsin sequences, expression patterns, and functions seen today depends critically on understanding the interactions among these groups (Porter et al., 2012). C-opsins are present in vertebrates, while R-opsins are found in arthropods and cephalopods, and cnidopsins are found exclusively in Cnidaria (ex. Jellyfish); which do not have light sensing organs but have some photosensitivity capabilities. Group 4 opsins are divergent opsins, since they are non-visual opsins but are believed to be tied to circadian rhythm processes. Gene duplication events have led to the vast diversity of opsins in the animal kingdom, and an equally diverse array of light sensitivities (Fig. 8).

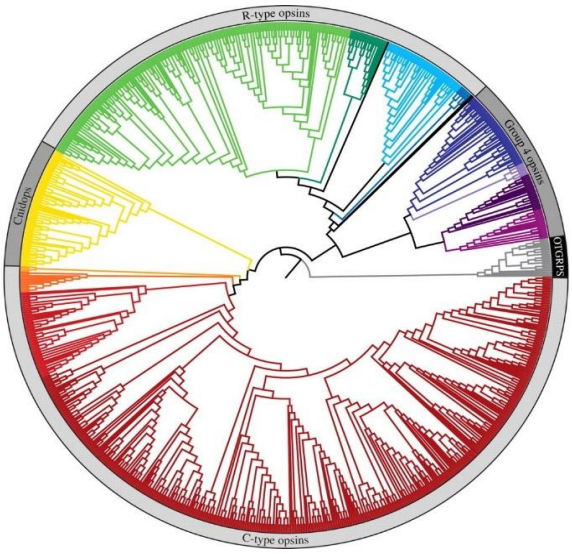

Figure 8. Maximum-likelihood tree of 889 expressed and genomic opsin sequences.

The four main opsin clades have been identified, and the branches of significant phylogenetic groups and subgroups have been colored. The outer circle representing outgroups has been colored

black, and the branches of the tree representing closely related non-opsin GPCRs have been colored grey. Adapted from Porter et al., 2012.

Rhabdomeric photoreceptors contain R-opsins, which depolarize utilizing a Gq-type signal transduction route. It is common for "R-type" photopigments to be bistable, keeping the chromophore in both the native (dark) and photoactivated (light) states (Porter et al., 2012). On the other hand, ciliary photoreceptors (such as the vertebrate rods and cones) have C-opsins that respond to light by hyperpolarizing, which is started by a Gt (transducing)-mediated signaling cascade (Porter et al., 2012). After being photoactivated, "C-type" photopigments lose their bound chromophore and bleach.

The evolution of light sensing and photoreception in animals can be better understood by looking at the evolutionary history of opsins. It is now possible to analyze opsins that are less well described histologically and functionally and to study the evolution of opsins exclusively from a genetic standpoint because of the appearance and rapid expansion of genomic data (Porter et al., 2012). Since the first sequences became accessible, the evolutionary history of the opsins has attracted a lot of attention. Nevertheless, studies of the function of the visual pigments have continued to use a small number of model organisms (such as zebrafish, mice, cows, and fruit flies), and most studies have only considered the opsins expressed in retinal tissues (Porter et al., 2012).

Moreover, while some recent studies have explored the diversity of opsins in different groups of insects, they tend to focus on the more “popular” insect orders (e.g.; *Odonata* and *Lepidoptera*) and tend to leave behind the “ugly stepchildren” insect orders (e.g.. *Mecoptera* and

Mantodea). For example, Futahashi, et al. characterized 20 opsin genes in the group *Libellulidae* (dragonflies) (2015) and Henze et al. described the expression pattern of opsins in the compound eye of *Gryllus* (crickets) (2012). Despite this recent work, large gaps remain in our understanding of both the evolution of insect opsins and their diversity across major groups of insects. Our goal was to expand our sampling of insect opsins and then use these new data to explore and better understand patterns of evolution and diversity of these crucial genes.

CHAPTER IV

MORPHOLOGY OF BISTANTA MEXICANA

This work focuses on the mantis *Bistanta* mexicana, as it is a native species of the Rio Grande Valley and represents the understudied insect order *Mantodea*.

The Sonoran Desert of Arizona, the tropical mountains of Guerrero, and even the southern plains of Texas are all part of the vast distribution range of the genus Bistanta. It has now been established through additional research on sampling material from these various areas that Bistanta is made up of five distinct species that have been taxonomically mixed up throughout the past century under various names (Anderson, 2022).

Male pronotal length to supracoxal dilation width is 5.95mm in length, pronotal length to minimal metazonal width is 7.81mm in length, metazona length to prozona length is 1.94mm, and supracoxal dilation width to minimal metazonal width is 1.31mm in length (Anderson, 2018). The supraanal plate is 1.26 times as long as the basal plate. Light gray softly infumates from the wings (Anderson, 2022). Female pronotal length to supracoxal dilation width is 6.10mm; pronotal length to minimal metazonal width is 7.48mm; prozona length to metazona length is 2.64mm; and supracoxal dilation width to minimal metazonal width is 1.23mm (Anderson, 2022). The supraanal plate is 1.39 times as long as the basal plate (Fig. 9).

Figure 9. Adult *B. mexicana*.

(A) Adult male found in Mazatlan, Sinaloa, Mexico. (B) Adult female found in Mazatlan, Sinaloa, Mexico. Adapted from Anderson, 2018.

Adults of the species *Bistanta mexicana* have three oval dorsal ocelli on the heads and a pair of elliptical compound eyes (Fig. 10) Under normal circumstances, the compound eyes do not have pseudopupils and are brown with white striations. The compound eyes do not exhibit any significant sexual dimorphism or regional differences that can be seen with microscopic examinations.

Figure 10. Light microscopy of general morphology of *B. mexicana*.

Image taken with Leica dissecting microscope.

Confocal microscopy of the eye of the mantis *Bistanta mexicana* revealed there is no spacing present between the tip of the crystalline cone and the tip of the rhabdom, making it an apposition compound eye (Fig. 11).

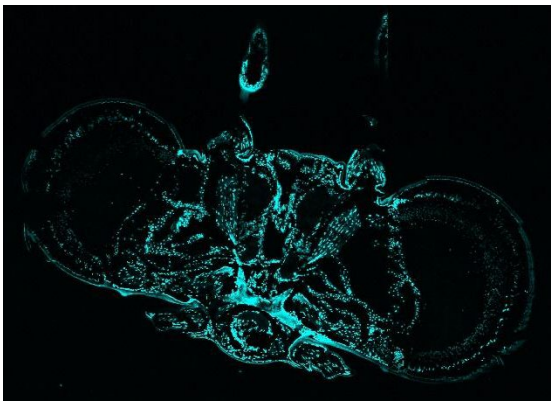

Figure 11. Confocal microscopy of the general morphology of *B. mexicana*.

Image taken with UTRGV's confocal microscope and DAPI stain.

CHAPTER V

METHODOLOGY

Specimen Collection

Specimens of the insect orders Collembola (*Hypogasturidae*, Springtails); Dermaptera (*Doru taeniatum*, Earwigs); Ephemeroptera (*Hexagenia limbata*, Mayflies); Embiidina (*Xenylla*, Webspinners); Mecoptera (*Panorpa dubia*, Scorpionflies); Neuroptera (*Dicromantispa sayi*, Net-winged insects); Phasmatodea (*Diapheromera tamaulipensis*, Stick insects); Zygentoma (*Thermobia*, Silver fish); and Plecoptera (*Perlesta placida*, Stoneflies) were collected throughout Central and South Texas. Specimens of the native praying mantis *Bistanta mexicana* (Mantodea) were collected at lights located at City of Mission Hike and Bike Trail Park. This site has an extensive natural area and is located two miles north of the border with Mexico and Bentsen-Rio Grande Valley State Park; an even larger partially conserved natural area. The specimens were starved for 2 days following capture to allow for the natural processing of previously eaten prey and prevent contamination by foreign genetic material.

RNA Extraction and Sequencing

This project expanded the available hexapod opsins by sampling eight additional orders: *Collembola*, *Dermaptera*, *Ephemeroptera*, *Mantodea*, *Mecoptera*, *Neuroptera*, *Phasmatodea*, and

Plecoptera. This represents a dramatic increase in sampling at the ordinal level and allowed us an in-depth analysis of insect opsin evolution. Trizol extractions of RNA from species of these orders native to central and south Texas using the Invitrogen Kit. The RNA samples were sent to Illumina for next-generation sequencing.

Transcriptome Assembly

The RNA samples were sent to Novogene for library synthesis and sequencing on the Illumina HiSeq (Böhm et al. 2018). Then, we assembled *De novo* transcriptomes using the Trinity pipeline (Hass et al., 2013) on the UTRGV High Performance Computing Cluster and identified opsin homologs via local BLAST search on each assembled transcriptome. Positively identified homologs were added to currently available insect opsin sequences (mainly *Drosophila*). Sequence alignment of amino acids was performed in MAFFT (Katoh et al., 2019).

At this point in the project, I decided to focus on the insect order *Mantodea* to which the model organism *Bistanta mexicana* belongs. The alignments of *B. mexicana* were then annotated and the phylogenetic relationships of the identified *B. mexicana* (Bm) transcripts were assessed in both PAML (Yang, 2007) and MrBayes (Ronquist et al., 2012).

Identification of Opsin Transcripts

Primers were designed using the Primer3 platform. Considering the results of the sequence alignment and gene annotation, primers were designed for the 4 full-length visual opsins (Bm42, Bm11, Bm 35 and Bm61); 3 full-length non-visual opsins (BmPer, BmArth, and BmPter); and 2

of the partial visual opsin candidates (Bm24 and Bm25). The primers were ordered from Integrated DNA Technologies (IDT).

A trizol RNA extraction was performed from new specimens, followed by quantification using NanoDrop spectroscopy, followed by cDNA synthesis using the Invitrogen kit.

The primers were then validated via PCR, with all nine of the primers successfully amplifying the cDNA samples. The PCR products of these were amplified using Taq polymerase and their corresponding primers, to generate sufficient PCR product samples for gene cloning.

Gene cloning and Verification

Gene cloning was performed using the Invitrogen Dual Promoter TOPO TA Cloning Kit. The standard protocol was followed except for it being scaled down to ¼ reactions. The PCR products of Bm25, Bm 11, Bm42, Bm 35 , Bm 24, Bm61, BmPter, BmArth and BmPer were ligated into the pCRII vector. Then we transformed our ligation products into One Shot TOP10 Chemically Competent E. coli via heat-shock. The transformed bacteria were plated into kanamycin plates and incubated overnight at 36˚C. Then, positive cloning screening was undertaken by sampling 10-12 colony forming units (CFUs) for each gene through color verification (white CFUs indicate positive insertion, while blue CFUs should be avoided). Initial verification of successful cloning was performed using the sampled CFUs and the designed primers through PCR amplification. Reference plates were also prepared using the sampled CFUs and stored indefinetly for future use at 4˚C. A second verification through another PCR amplification performed by using the MI3 and designed primers to check for a difference in PCR product size. If the cloning was successful, we would expect the MI3 products to be about 250bp

larger than the designed primer products. The BmArth clones did not pass the second verification, so it was decided to not continue with them in the next phase. Moreover, since the PCR product can ligate into the vector in either orientation, we also sent the individual recombinant plasmids to Illumina to analyze for the presence and orientation of the PCR product by next-generation sequencing.

After a satisfactory second verification of successful cloning, we proceeded to further amplify the eight Bm candidate genes (Bm25, Bm 11, Bm42, Bm 35, Bm 24, Bm61, BmPter and BmPer) through PCR, in order to have sufficient template to isolate the plasmid cDNA. Ethanol DNA precipitation was performed to isolate the plasmid cDNA and generate probes following standard protocol. DNA quantification was performed via NanoDrop spectroscopy. All samples were diluted in RNAse free water to reach the final concentration of 200ng/μL.

Bistanta mexicana Head Fixation, Rehydration and Sectioning

The protocol for Henze et al. (2012) was followed for the head fixation, rehydration, and sectioning described below.

Head Fixation

Heads were dissected and stored in 4% formaldehyde for 30 minutes with rocking. The heads were washed with 1X PBS (phosphate-buffered saline) and serially diluted into MeOH for indefinite storage at -20˚C.

Rehydration

The heads were serially rehydrated using 1X PBS. The tissue was then serially incubated in: 10% sucrose for 5 minutes with rocking; 20% sucrose for 5 minutes with rocking; 30% sucrose for 5 minutes with rocking; 1:1 O.C.T.:30% sucrose solution for 30 minutes with rocking (Tissue-Tek O.C.T. Compound, Sakura Finetek Europe B.V.); and 100% O.C.T. overnight (16-18 hrs).

Sectioning

The heads embedded in freezing medium (O.C.T.) at -20˚C and 20 µm thick sections were cut on the UTRGV cryostat (Microm HM 550, Thermo Fisher Scientific Inc.). Sections were mounted on electrostatically charged slides (SuperFrost Plus Slides, Thermo Fisher Scientific Inc.) and dried at room temperature.

Fluorescent *In Situ* Hybridization in *B. mexicana* Eye Sections Using Tyramide Signal Amplification

In vitro transcription to generate probes

Due to time constraints, it was decided to select only three Bm opsin candidates to continue into the probe generation phase. The three Bm opsins chosen were Bm11, Bm42, and Bm61 based on their sequence similarity to represent the three major types of wavelength sensitivity. While it is advised to only synthesize antisense probes due to cost expenses, because of time constraints and the lack of sequencing results of the recombinant plasmids, we decided to go ahead and transcribe both the Sp6 and T7 probes to define the insert orientation through signaling verification

via antibody detection using tyramide during an initial assay. This initial viability assay confirmed the insert orientation, with Bm11 Sp6, Bm42Sp6 and Bm61T7 being the antisense probes. From that point on, these antisense probes were used to characterize the spatial localization of the Bm opsins in the compound eye of *B. mexicana*. The protocol by Jandura et al. (2017) was followed.

4 µL of PCR product (linearized plasmids containing a cDNA fragment of the respective Bm opsin gene) and the DIG RNA master mix (DIG RNA labeling kit, Roche Diagnostics) were incubated at 37 °C for 3.5-4 hours to transcribe the antisense digoxigenin (DIG) labeled RNA probes (Bm11 Sp6, Bm42Sp6 and Bm61T7). The synthesized probes (15µL) were mixed with 35 µL of DEPC treated ddH2O, 125 µL of 100 % EtOH, and 5 µL of 3 M NaOAC (pH=5.2, RNase free). The probes were then stored at -80 °C for at least 30 minutes. Afterwards, the probes were centrifuged at 14,000 RM and 4°C for 20 minutes. Then the probes were washed once with cold 75% EtOH and centrifuged at 14,000 RM and 4°C for 2 minutes. The probes were air dried for 6 minutes, and then the precipitated probes were resuspended in 25 µL of DEPC treated ddH2O. 5 µL of each probe was ran on a 1% agarose gel to check the integrity and yield of the probes. The remaining 20 µL of the synthesized probe were mixed with 100 µL hybridization solution and stored at -80 °C indefinitely.

In situ Hybridization

The protocol by Jandura et al. (2017) was followed. Sections were rehydrated by adding 50 µL PBTT (1 X PBS, 0.1 % Tween-20, and 0.3% Triton-X-100) and incubated for 1 minute. A working Protk (2.667 µg/mL) solution was prepared and the tissues were incubated in 50 µL of working Protk solution for 6 minutes. Working glycine (2mg/mL) solution was prepared and the

tissues were washed 3 times with 50 µL of working glycine solution for 2 minutes each. Tissues were then washed 3 times with 50 µL of PBTT. Sections were incubated in 50 µL of 4% PFA for 20 minutes. Hybridization Buffer was prepared according to the protocol by Jandura et al. (2017), and boiled for 5 minutes, and then cooled on ice immediately for 5 minutes. Tissues were washed 3 times with 50 µL PBTT for 2 minutes each. Then we washed once with 50 µL of 1:1 PBTT: Hyb. Buffer solution. Sections were then washed twice with 50µL of Hybridization Buffer. Tissues were incubated in Hybridization Buffer at 56˚C for 2.5-3 hrs. Working probe was prepared by adding 10µL of probe to 90µL of Hybridization Buffer. The working probes were incubated in the thermocycler at 80˚C for 5 minutes, and then cooled on ice. The tissues were incubated in working probe and at 56˚C overnight (16-18 hrs).

Probe detection

The protocol by Jandura et al. (2017) was followed. Prepared post-hybridization solutions and pre-warmed them to 56˚C. Washed probes twice with 110µL of post-hybridization 3:1 Hybridization Buffer:PBTT solution at 56˚C for 15 minutes each. Washed probes with 110µL of post-hybridization 1:1 Hybridization Buffer:PBTT solution at 56˚C for 15 minutes. Washed probes with 110µL of post-hybridization 1:3 Hybridization Buffer:PBTT solution at 56˚C for 15 minutes. Washed probes three times with 110µL of PBTT at 56˚C for 5 minutes each. Then, the probes were removed from the incubator and allowed to cool down to room temperature.

Primary antibody solution (2.5µg/mL) was prepared by adding 2µL of biotin-conjugated mouse monoclonal anti-DIG antibody (Thermo Fisher Scientific Inc.) and 800µL of PBTTB (1 % Skim milk in 1 X PBTT). Streptavidin-HRP solution (1µg/mL) was prepared by adding 1µL

of streptavidin-HRP conjugate (Thermo Fisher Scientific Inc.) to 1000µL of PBTTB. Tissues were blocked with 100µL of PBTTB for 20 minutes, and then incubated in 100µL of primary antibody solution for 2 hours at room temperature. Tissues were washed twice with 100µL of PBTTB. The tissues were washed three times with 100µL of PBTTB for 5 minutes each. Washed five times with 100µL of PBTTB for 10 minutes each. Incubated tissues in streptavidin-HRP solution for 1.5 hours at room temperature. Washed tissues twice with 100µL of PBTTB for 5 minutes each. Kept tissues in dark from this point on.

Antibody Detection Using Tyramide and Confocal Microscopy

The protocol by Jandura et al. (2017) was followed. Prepared tyramide activation buffer containing 0.006 % of H_2O_2 in PBTT by adding 3µL of 3% H_2O_2 into 1,500µL of 1X PBTT. Washed tissues with 100µL of tyramide activation buffer. Prepared cyanine 3 (cy3)-tyramide solution by adding 2µL of stock cy3-tyramide (1.12 mM/mL, Invitrogen) to 1,000µL of activation buffer. Prepared cyanine 5 (cy5)-tyramide solution by adding 2µL of stock cy5-tyramide (1.12 mM/mL, Invitrogen) to 1,000µL of activation buffer. Tissues hybridized with the Bm42 and Bm61 probes were incubated in cy3-tyramide solution, while tissues hybridized with Bm11 were incubated in cy5-tyramide solution. All tissues were incubated in the cyanine-tyramide solution for 8 minutes at room temperature and always kept in the dark. Tissues were washed three times with 100µL of PBTT. Incubated tissues in 1:500 DAPI solution for 15 minutes. Washed four times with 100µL of PBTT for 10 minutes each. Washed three times with 100µL of PBS for 5 minutes each. Added 1 drop of antifade mounting media. Covered with coverslip and sealed the edges of the coverslip with nail polish. Imaged using a fluorescence microscope at UTRGV.

CHAPTER VI

RESULTS AND DISCUSSION

RNA Extraction and Sequencing Results

RNA was successfully collected for all eight insect orders, and we obtained their transcription data after next-generation sequencing by Illumina.

Transcriptome Assembly Results

Preliminary sequence alignment results were obtained for 7 of our insect orders: *Collembola*, *Dermaptera*, *Ephemeroptera*, *Mecoptera*, *Neuroptera*, *Phasmatodea*. Future research in the Terry lab will focus on using the generated preliminary data for the understudied seven insect orders (*Collembola*, *Dermaptera*, *Ephemeroptera*, *Mecoptera*, *Neuroptera*, *Phasmatodea*) to assess gene duplication events and evolution across the insects in the context of previously established insect relationships (Misof et al., 2014). Using enlarged alignments will make it possible to identify differential selection pressures on both amino acid residues and different regions of the opsin gene.

Identification of Opsin Transcripts Results

Through sequence allignment and gene annotation, 9 opsin homologs were found: 4 full-length visual opsins (Bm42, Bm11, Bm35 and Bm61); 3 full-length non-visual opsins (BmPer, BmArth, and BmPter); and 2 partial visual opsin candidates (Bm24 and Bm25).

The phylogenetic relationships analysis of the *B. mexicana* transcripts yielded a preliminary opsin gene phylogeny for *B. mexicana* (Fig. 12).

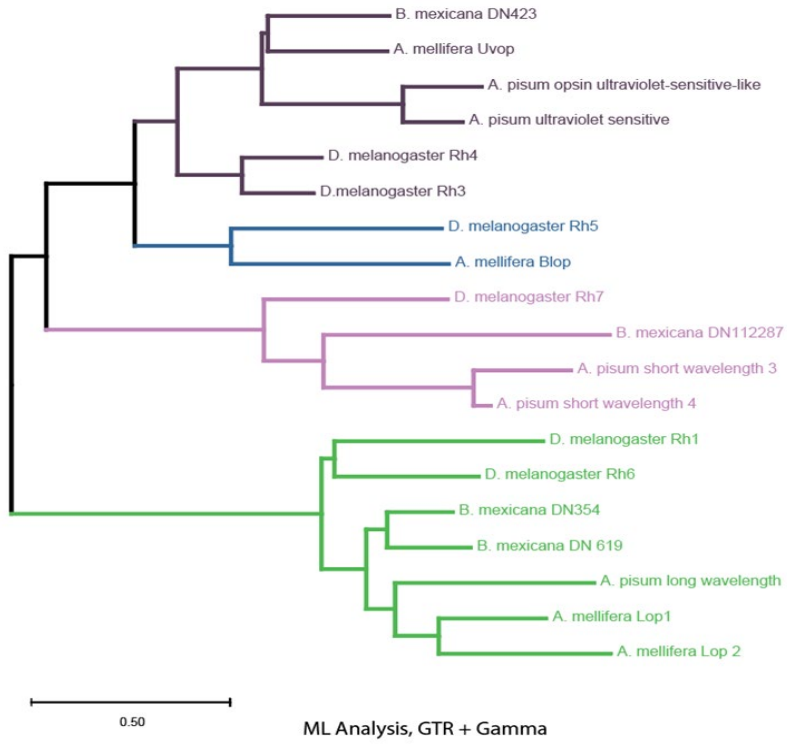

Figure 12. Gene phylogeny of 4 full-length Bm visual opsins.

Phylogeny depicts the 4 full-length Bm visual opsins and *Drosophila* opsin homologs. Based on sequence similarity the Bm homologs were classified as short-wavelength (pink), middle-wavelength (blue), long-wavelength (green) and non-visual (black).

All six Bm visual opsin homologs were categorized into a wavelength sensitivity category according to their sequence similarity compared to well-studied *Drosophila* homologs (Table 1).

Table 1. Bm visual opsins' sequence similarity.

SW (UV-sensitive)	MW (blue-sensitive)	LW (blue to violet-sensitive)
Bm42	Bm11	Bm25
		Bm61
		Bm24
		Bm35

Gene cloning and Verification Results

The initial PCR verification of the nine Bm cloned genes using our designed primers was satisfactory, but we still wanted to perform a second verification through another PCR amplification using the MI3F/R primers and comparing the MI3 products to the designed primers products. The PCR products of Bm11, Bm24, BmPter, BmArth and BmPer can be seen in Fig. 13.

Of the nine primers designed, eight of them successfully passed the second PCR validation process and led to the isolation of PCR products that became candidates for cloning. The candidates selected for cloning were Bm25, Bm 11, Bm42, Bm 35, Bm 24, Bm61, BmPter and BmPer. The BmArth clones did not pass the second verification, so it was decided to not continue with them in the next phase. Furthermore, the individual recombinant plasmids were sent to Illumina to analyze for the presence and orientation of the PCR product by next-generation sequencing. The sequencing results are pending, but the results will be incorporated into the lab's

future research. The plasmid cDNA of all eight clones was successfully isolated via ethanol DNA precipitation, allowing us to generate probes.

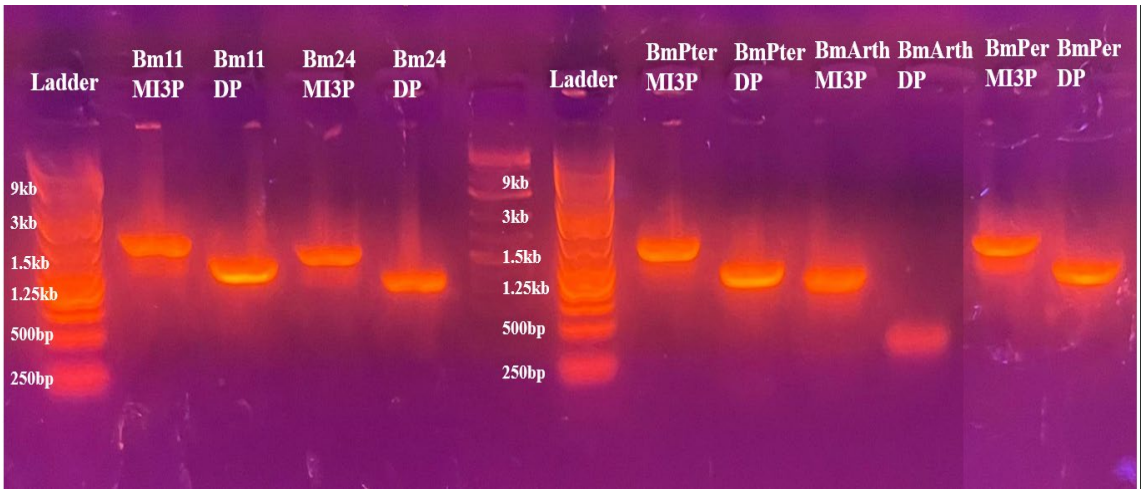

Figure 13. PCR verification of successful cloning of target opsin genes.

The MI3 products are about 250bp larger than the designed primers products, being a satisfactory indicator of successful cloning of the 8 Bm clones opsin genes (Bm25, Bm 11, Bm42, Bm 35, Bm 24, Bm61, BmPter and BmPer). BmArth was not a successful clone.

In vitro transcription to generate probes Results

Only three Bm opsin candidates were chosen to go into the probe creation phase due to time restrictions. The three Bm opsins chosen were Bm11, Bm42, and Bm61 based on their sequence similarity to represent the three major types of wavelength sensitivity. To assess the integrity and yield of the probes, 5 µL of each probe was run on a 1% agarose gel. The gel results showed a satisfactory probe generation of Bm11Sp6, Bm42 Sp6, Bm42 T7, Bm61 Sp6 and Bm61 T7 (Fig. 14). Bm11 T7 lacked a band for the RNA probe, so it was not moved into the next phase.

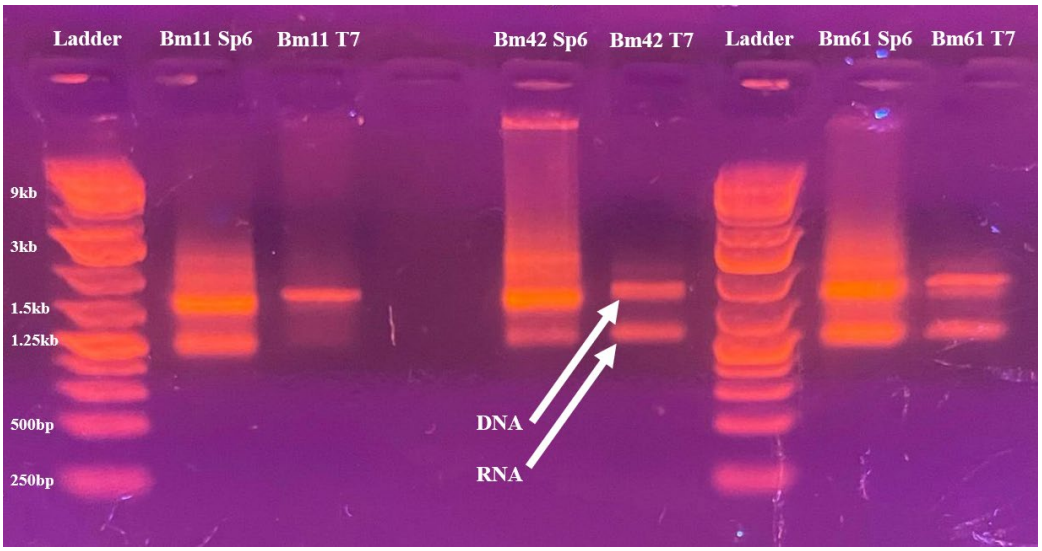

Figure 14. Gel electrophoresis of synthesized DIG-labeled probes.

Newly synthesized RNA probes observed on a 1 % agarose gel (5 µL/lane). The yield can be categorized (based on the intensity of the band) as 'low yield' for Bm61 T7 and 'typical yield' for Bm42 T7, or 'high yield' for Bm11 Sp6, Bm42 Sp6, and Bm61 Sp6. The arrow points to one of the 'RNA probes', the higher band on each lane is the original DNA template. Bm11 T7 lacked a band for the RNA probe.

In Situ Hybridization and Confocal Microscopy Results

Confocal microscopy of the sections hybridized with Bm11, Bm42 and Bm61 probes all yielded a signal. It was interesting to observe how Bm42 (SW opsins, UV-sensitive), Bm11 (MW, blue-sensitive), and Bm61 (LW opsin, blue to violet-sensitive) were localized in the lower end of the photoreceptor cells (Fig. 15). More interestingly, there was expression of all three opsin genes in brain tissue. Future work should focus on troubleshooting off-target binding of tyramide and autofluorescence of DAPI.

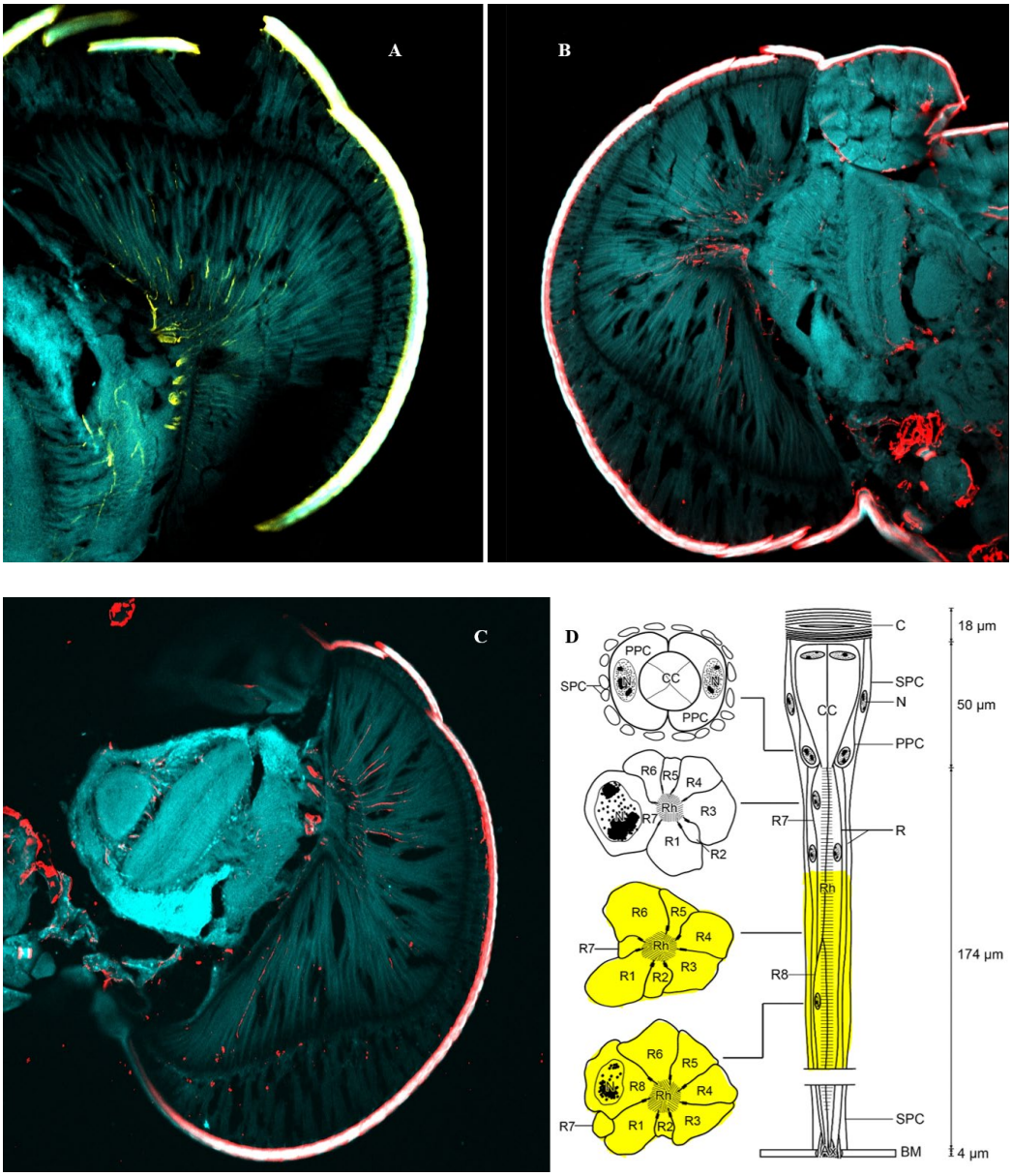

Figure 15. Confocal microscopy of hybridized *B. mexicana* eye sections.

(A) Bm11 opsin gene was stained with cy5-tyramide and is shown in yellow. (B) Bm42 opsin gene was stained with cy3-tyramide and is shown in red. (C) Bm61 opsin gene was stained with cy3-tyramide and is shown in red. (D) All three opsin genes are localized in the lower dorsal area of the compound eye, presumably in the lower ends of the photoreceptor cells. Diagram adapted from Chen and Hua (2016).

REFERENCES

Anderson, Kris. (2022). Revision of the North American Genus Bistanta Anderson, 2018. 3. 1-47. 10.5281/zenodo.6533412.

Chen, Q. X., & Hua, B. Z. (2016). Ultrastructure and Morphology of Compound Eyes of the Scorpionfly Panorpa dubia (Insecta: Mecoptera: Panorpidae). PloS one, 11(6), e0156970. https://doi.org/10.1371/journal.pone.0156970

Erclik, T., Hartenstein, V., McInnes, R. R., & Lipshitz, H. D. (2009). Eye evolution at high resolution: the neuron as a unit of homology. Developmental biology, 332(1), 70–79. https://doi.org/10.1016/j.ydbio.2009.05.565

Futahashi, R., Kawahara-Miki, R., Kinoshita, M., Yoshitake, K., Yajima, S., Arikawa, K., & Fukatsu, T. (2015). Extraordinary diversity of visual opsin genes in dragonflies. Proceedings of the National Academy of Sciences of the United States of America, 112(11), E1247–E1256. https://doi.org/10.1073/pnas.1424670112

Gehring W. J. (2014). The evolution of vision. Wiley interdisciplinary reviews. Developmental biology, 3(1), 1–40. https://doi.org/10.1002/wdev.96

Henze, M. J., Dannenhauer, K., Kohler, M., Labhart, T., & Gesemann, M. (2012). Opsin evolution and expression in arthropod compound eyes and ocelli: insights from the cricket Gryllus bimaculatus. BMC evolutionary biology, 12, 163. https://doi.org/10.1186/1471-2148-12-163

Jandura, A., Hu, J., Wilk, R., & Krause, H. M. (2017). High Resolution Fluorescent In Situ Hybridization in Drosophila Embryos and Tissues Using Tyramide Signal Amplification. Journal of visualized experiments : JoVE, (128), 56281. https://doi.org/10.3791/56281

Katoh, K., Rozewicki, J., & Yamada, K. D. (2019). MAFFT online service: multiple sequence alignment, interactive sequence choice and visualization. Briefings in bioinformatics, 20(4), 1160–1166. https://doi.org/10.1093/bib/bbx108

Koenig, K. M., & Gross, J. M. (2020). Evolution and development of complex eyes: a celebration of diversity. Development (Cambridge, England), 147(19), dev182923. https://doi.org/10.1242/dev.182923

Misof, B., Liu, S., Meusemann, K., Peters, R. S., Donath, A., Mayer, C., Frandsen, P. B., Ware, J., Flouri, T., Beutel, R. G., Niehuis, O., Petersen, M., Izquierdo-Carrasco, F., Wappler, T., Rust, J., Aberer, A. J., Aspöck, U., Aspöck, H., Bartel, D., Blanke, A., … Zhou, X. (2014). Phylogenomics resolves the timing and pattern of insect evolution. Science (New York, N.Y.), 346(6210), 763–767. https://doi.org/10.1126/science.1257570

Porter, M. L., Blasic, J. R., Bok, M. J., Cameron, E. G., Pringle, T., Cronin, T. W., & Robinson, P. R. (2012). Shedding new light on opsin evolution. Proceedings. Biological sciences, 279(1726), 3–14. https://doi.org/10.1098/rspb.2011.1819

Ronquist, F., Teslenko, M., van der Mark, P., Ayres, D. L., Darling, A., Höhna, S., Larget, B., Liu, L., Suchard, M. A., & Huelsenbeck, J. P. (2012). MrBayes 3.2: efficient Bayesian phylogenetic inference and model choice across a large model space. Systematic biology, 61(3), 539–542. https://doi.org/10.1093/sysbio/sys029

Shichida, Y., & Matsuyama, T. (2009). Evolution of opsins and phototransduction. Philosophical transactions of the Royal Society of London. Series B, Biological sciences, 364(1531), 2881–2895. https://doi.org/10.1098/rstb.2009.0051

Spaethe, J., & Briscoe, A. D. (2005). Molecular characterization and expression of the UV opsin in bumblebees: three ommatidial subtypes in the retina and a new photoreceptor organ in the lamina. The Journal of experimental biology, 208(Pt 12), 2347–2361. https://doi.org/10.1242/jeb.01634

Terakita, A. (2005). The opsins. Genome biology, 6(3), 213. https://doi.org/10.1186/gb-2005-6-3-213

Warrant, E. J., & Locket, N. A. (2004). Vision in the deep sea. Biological reviews of the Cambridge Philosophical Society, 79(3), 671–712. https://doi.org/10.1017/s1464793103006420

Yang, Z. (2007). PAML 4: phylogenetic analysis by maximum likelihood. Molecular biology and evolution, 24(8), 1586–1591. https://doi.org/10.1093/molbev/msm088

BIOGRAPHICAL SKETCH

Maria Jose Cardenas Muedano was born and raised in Mexico City. She decided to complete her undergraduate education in the United States to have more research opportunities in the field of Molecular Biology. She graduated from St. Edward's University in Austin, TX with a Bachelor of Science in Biology in May 2020. She then completed her Master of Science in Biology at The University of Texas Rio Grande Valley (UTRGV) in Edinburg, TX in December 2022. This thesis was part of her MS in Biology degree.

Maria Jose is currently working as a teaching assistant and lab technician at UTRGV and is planning to pursue a doctorate degree in Molecular and Cellular Biology soon. She is interested in phylogenomics, evo-devo and entomology; as a result, she engages in a lot of outdoor activities such as insect specimen collections around Texas and abroad. Maria Jose is married and lives with her wife and three dogs in Edinburg, TX.

For questions related to this thesis, please contact Maria Jose at mjcmuedano@gmail.com.